



Acta Scientiarum. Technology

ISSN: 1806-2563

eduem@uem.br

Universidade Estadual de Maringá

Brasil

Gouvêa Melo, Aurélio; Oliveira Filho, Delly; Martins de Oliveira Júnior, Maury; Zolnier, Sérgio; Ribeiro, Aristides

Development of a closed and open loop solar tracker technology

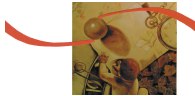
Acta Scientiarum. Technology, vol. 39, núm. 2, abril-junio, 2017, pp. 177-183

Universidade Estadual de Maringá

Maringá, Brasil

Available in: <http://www.redalyc.org/articulo.oa?id=303250905007>

- ▶ How to cite
- ▶ Complete issue
- ▶ More information about this article
- ▶ Journal's homepage in redalyc.org



Development of a closed and open loop solar tracker technology

Aurélio Gouvêa Melo, Delly Oliveira Filho*, Maury Martins de Oliveira Júnior, Sérgio Zolnier and Aristides Ribeiro

*Universidade Federal de Viçosa, Av. Peter Henry Rolfs, s/n, 36570-900, Viçosa, Minas Gerais, Brazil. *Author for correspondence. E-mail: delly@ufv.br*

ABSTRACT. Solar energy is among the renewable energy sources that received greater addition in installed capacity. However, it accounts for a small fraction of the energy matrix of most countries. Electric energy generation by solar systems can be improved through tracking. This work aimed to develop and compare a closed and an open loop solar tracking system. The closed loop system was developed using Light Dependent Resistors. An algorithm was developed for the open loop tracker as a function of the geometric relation between the sun and the photovoltaic module. A simulation was run to compare this algorithm with a system using tracking at fixed time intervals, for clear sky conditions, with different tracking parameters and for five different latitudes. No significant difference was observed between the proposed open loop tracking algorithm and the fixed time interval algorithm for the tracking parameters evaluated. The open and closed loop solar tracking systems were compared experimentally in Rio das Ostras, Brazil (22.49 °S 41.92° W). An average gain of 28.5% was observed for the open loop tracking system over a latitude tilted system and 33.0% for the closed loop tracking system.

Keywords: solar energy, dual axis tracking, photovoltaic systems.

Desenvolvimento de tecnologia de rastreamento solar com controle em malha fechada e em malha aberta

RESUMO. A energia solar está entre as fontes de energia com maior incremento em sua capacidade instalada, mas ainda representa uma pequena fração da matriz energética mundial. A geração de energia a partir de sistemas fotovoltaicos pode ser melhorada por meio do rastreamento solar. O objetivo deste trabalho foi desenvolver e comparar sistemas de rastreamento solar com controle em malha aberta e malha fechada. O sistema com malha fechada foi desenvolvido utilizando resistores dependentes da luz. Um algoritmo de rastreamento em malha aberta foi desenvolvido com base na relação geométrica entre o sol e o módulo fotovoltaico. Este algoritmo foi comparado com um algoritmo de rastreamento a intervalos fixos de tempo por meio de simulação para condição de céu claro e para cinco latitudes. Não foi observada diferença significativa entre o algoritmo desenvolvido e o rastreamento em intervalos fixos de tempo para os casos avaliados. Os sistemas de rastreamento em malha aberta e malha fechada foram comparados experimentalmente para a cidade de Rio das Ostras, Brasil (22,49°S 41,92°O). Foi observado um aumento médio de 28,5 e 33,0% para os sistemas de rastreamento em malha aberta e malha fechada, respectivamente, em relação a um sistema fixo com inclinação igual à latitude.

Palavras-chave: energia solar, rastreamento biaxial, sistemas fotovoltaicos.

Introduction

A growing demand for electrical power due to its transformation flexibility has been observed in modern society. In this context, solar energy has obtained a prominent function in several countries such as Germany, China, Japan and others, mainly due to its clean matrix and possibility of distributed installation (Renewable Energy Policy Network for the 21st Century [Ren21], 2016).

The benefits of a photovoltaic generator include (i) Sustainable technology, (ii) Availability of solar radiation, (iii) Low installation impact on the environment, (iv) Lifespan over 15 years, (v) Low

maintenance requirements, (vi) Modularity, (vii) Possibility of installation near the load centers, and (viii) Noiseless and emission-free operation.

Despite its advantages, the cost and efficiency of photovoltaic generation are not usually as competitive as other energy sources, such as hydroelectric generation. Thus, several methods are proposed in literature to improve photovoltaic power generation performance, thereby enhancing the cost/benefit relationship.

Due to variations in the available instantaneous solar irradiance throughout the daylight period, the solar cells generally have an average efficiency of about 20% of its capacity (Mousazadeh et al., 2009).

One of the most important factors about the generator performance is the sunlight incidence angle, which depends on the generator geographic location, daytime, day of the year and weather conditions (Lubitz, 2010).

The energy available for conversion in a photovoltaic generator can be increased throughout the day by methods to track the sun position, keeping the system perpendicular to the solar beam radiation. In flat panel generators, it is possible to use 98% of the system capacity just by using tracking devices with errors between the generator and the sun direction of up to 10% (Guo, Cha, Liu, & Tian, 2010).

Few solar power plants actually in operation have tracking systems, with either one or two axis, however there are applications of tracking in large scale power plants. The Nellis airforce base in Nevada holds one of the largest photovoltaic plants in North America with 10 MWp capacity and one axis tracking system. On this site, the set of trackers allows for 50% increase in performance on cloudy days, when compared to fixed flat panels. (Kelly & Gibson, 2011). According to Gómez-Gil, Wang and Barnett (2012), about 24% of the Spanish systems have one axis tracking and 13% with two axis tracking, which presented a performance increase of about 22 and 25%, respectively, and thus, better economic feasibility. The local latitude is an important indicator of the maximum performance of the tracker. The theoretical boundaries are around 30% for one axis and around 50% for two axis tracking (Chin, Babu, & McBride, 2011).

There are two main methodologies to follow the sun across the sky, namely, open loop and closed loop systems. The first, open loop system, is based on the calculation of the solar position through mathematical models, so that the solar tracker can be positioned according to the results. The second methodology, i.e., closed loop, consists in the use of sensors to find the direction with the maximum amount of incident energy. This work aimed to compare these two solar tracking methodologies.

The present paper is organized as follows: Section II presents a brief review concerning solar radiation distribution. In Section III, the system and the applied methodology are proposed, while section IV presents and analyzes the results obtained. Section V presents the conclusions of the experiments.

Solar radiation distribution

The incident radiation on a surface can be decomposed into two components. The first is the direct beam radiation that comes from the sun and

can be mathematically calculated. The second component is the diffuse radiation, which arises from the scattering of light produced in the atmosphere due to reflection and absorption by air molecules.

Beam radiation usually conveys a greater amount of energy, compared to diffuse radiation. Therefore, the best orientation for a photovoltaic generator will be, in most cases, towards the beam component. In the case of cloudiness or in urban areas, such information may not be true due to possible solar reflections.

The diffuse radiation proportion is mainly affected by the intensity of radiation, light spectrum and incidence angle. These characteristics, along with the air layer thickness (air mass), determine the amount of energy in the diffuse component.

A simple analysis of the energy dispersion in the atmosphere can only be performed considering a clear sky. The presence of clouds strongly affects the dynamics of diffuse energy distribution by modifying the maximum intensity radiation point. However, sometimes the difference in the amount of received radiation might not be sufficient to justify moving the photovoltaic generator due to the energetic cost of this task.

The tracking operation can be described as follows. Open loop systems will perform sun position calculation regardless of cloudiness conditions and will position the generator based on the calculated values. The closed loop tracking systems will locate the best region according to the sun position, but the location of the point of maximum performance for solar energy will be based on the difference between sensor data.

In clear sky days, the beam solar radiation component accounts for over 85% of the total radiation and the remaining 15% is diffuse. However, on cloudy days, nearly all incident solar radiation is diffuse and performing solar tracking may not be feasible for maximizing energy capture, due to the energy spent to find the position of the sun (Yilmaz et al., 2015).

The trackers should be able to find the maximum radiation point regardless of the cloudiness condition. If considerable cloudiness occurs across all the celestial sphere, the maximum radiation point would occur in the less dense area. If the cloudiness were uniform, the best performance would occur with the generator positioned horizontally as it may not be feasible to move the tracker because of the amount of energy demanded. However, if only partial cloudiness conditions apply, better use should occur with orientation shifted a few degrees from the perpendicular direction of the sun rays.

The sky condition can be classified by the cloudiness index according to Table 1. This can be used as a reference for analysis of radiation data, although this index does not provide accurate information about cloud distribution, as it is determined by visual inspection resulting in a qualitative characterization.

Table 1. Cloudiness index (Wollmann & Sartori, 2010).

Index	Cloudiness condition
0	Clear sky
1 - 3	Low clouds
4 - 6	Mostly cloudy
7 - 9	Considerable cloudiness
10	Cloudy

Material and methods

The experimental system consists of two trackers, namely, the closed loop system, which is based on light sensor measurements; and the open loop system, based on sun position calculation. These devices were developed focusing on robustness, simplicity and efficiency.

A radiation meter on a horizontal surface and a fixed latitude tilted panel were used as reference. A calibration curve for the meter was obtained using a pyranometer in order to ensure the accuracy of the results. Performance evaluation was conducted for days with different cloudiness indexes obtained from the National Institute of Meteorology [INMET], (2014).

The experiments were performed in the city of Rio das Ostras, Brazil (22.49° S 41.92° W). The solar radiation index in the region is around $16 \text{ MJ m}^{-2} \text{ day}^{-1}$ or around $1,600 \text{ kW m}^{-2} \text{ year}^{-1}$ (Electrical Energy Research Center [CEPEL], 2000). The total solar radiation was collected in the horizontal plane by the solar radiation meter TES 1333R, which already has an integrated data logger function with the specifications presented in Table 2 (TES Electrical Electronic Corp., 2013). The calibration checkup was performed using a pyranometer CMP3 manufactured by Campbell with sensitivity factor of $12.15 \times 10^{-6} \text{ V W}^{-1} \text{ m}^{-2}$ (Campbell Scientific, 2013).

Table 2. Solar meter characteristics (TES Electrical Electronic Corp., 2013).

Parameter	Value
Range	0 to $2,000 \text{ W m}^{-2}$
Accuracy	$\pm 10 \text{ W m}^{-2}$
Memory	32,000 samples
Spectral response	400 - 1,100 nm
Temperature drift (25°C)	$\pm 0.38 \text{ W m}^{-2} \text{ }^{\circ}\text{C}^{-1}$
Aging	$< \pm 2\% \text{ year}^{-1}$

There are a few possible designs for the construction of light sensors. Three construction

methodologies were considered based on the results observed in the literature, namely a) lateral trims; b) central side trim; and c) with different slopes in the sensor planes (Hession & Bonwick, 1984; Prapas, Norton, & Proebert, 1986; Zogbi & Laplaze, 1984) shown in Figure 1. The light sensors used are Light Dependent Resistors (LDRs). Based on the literature, it seems that the central side trim is the most viable alternative, since it has more independent construction parameters, such as the sensor positioning angle and size of the trim.



Figure 1. Light sensor designs (a) lateral trim (b) central side trim and (c) with different slopes in the sensor planes.

As part of this research, an algorithm was developed to control the open loop tracking system in order to compare its efficiency with that of a system controlled by LDR sensors. This algorithm uses, as criteria to the reorientation of the panel, the variable d , i.e. as the value for this variable surpassed a predetermined limit, the system should be reoriented:

$$d = \sqrt{(\gamma_s' - \gamma_s)^2 + (\theta_z' - \theta_z)^2} \quad (1)$$

where,

γ_s = solar azimuth angle in the last reorientation of the system, $^{\circ}$;

γ_s' = actual solar azimuth angle, $^{\circ}$;

θ_z = zenith angle in the last reorientation of the system, $^{\circ}$; and

θ_z' = actual zenith angle, $^{\circ}$.

The algorithm used for the reorientation based on the LDR measurements is presented in Figure 2.

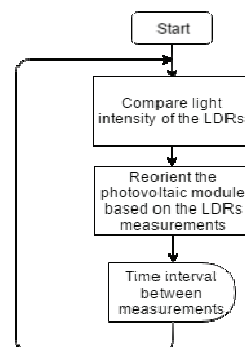


Figure 2. Simplified closed loop algorithm.

In order to evaluate the performance of this open loop algorithm for the orientation of the solar PV

system, this algorithm was compared with a simple and widely used tracking algorithm, i.e., the reorientation of the panel at fixed intervals of time, from sunrise to sunset, both with the same number of daily re-orientations. This comparison was made through the simulated radiation received by the solar panel surface throughout one year under clear sky conditions. The clear sky radiation on horizontal surface values were obtained with the use of the models proposed by Hottel and the model proposed by Liu and Jordan, as cited by Duffie and Beckman (2006). Then, the calculated values of beam, diffuse and total radiation were used in the anisotropic sky model of Perez, as cited by Duffie and Beckman (2006) to simulate the radiation received by the inclined surfaces.

Initially, the two algorithms, namely, the fixed time interval algorithm and the proposed open loop algorithm, were compared for the city of Rio das Ostras, where the experiments were conducted. Both algorithms were also compared to the radiation received by a horizontal and a surface with latitude tilt. The increase in radiation at the surface level by both algorithms was also observed as the number of mean daily re-orientations were altered. The fixed time interval and proposed algorithms are represented in the flowchart in Figure 3.

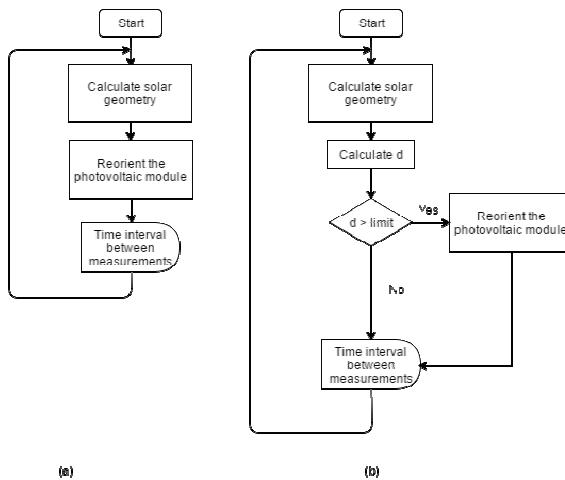


Figure 3. Simplified open loop algorithm for (a) the fixed time-interval and (b) proposed algorithms.

The increase in radiation for different latitudes was observed by the simulation of yearly radiation for five locations, as presented in Table 3.

Table 3. Latitude and altitude of simulated locations.

Location	Latitude (°)	Altitude (m)
Madison (USA)	43.07° N	270
Mexico City (Mexico)	19.33° N	2,268
Fortaleza (Brazil)	3.72° S	21
Rio das Ostras (Brazil)	22.29° S	13
Bariloche (Argentina)	41.15° S	836

Results and discussion

At first, the calibration curve of the radiation sensor was obtained. The obtained curve can be seen in Figure 4.

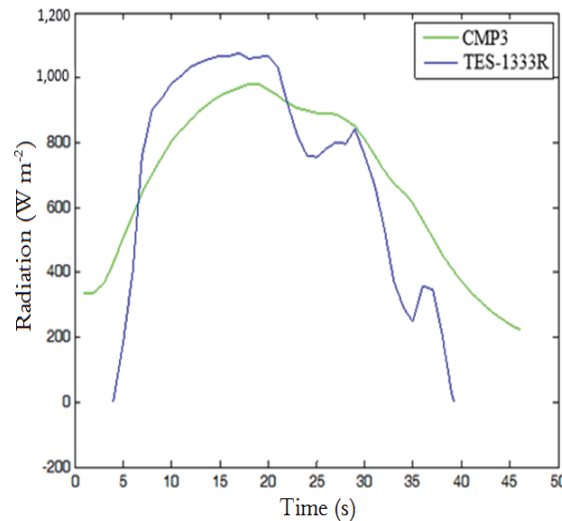


Figure 4. Measurements by pyranometer CMP3 (green) and by TES-1333R (blue) meter.

Equation 2 shows the linear regression for the same data. As observed, the main difference in the response of the sensors is related to the integration time, or, in other words, the response time of each sensor:

$$r_x = 0.53 r_i \quad (2)$$

where,

r_x = Calibrated radiation, (W m^{-2}); and

r_i = Radiation measured by TES-1333R meter, (W m^{-2}).

The fixed time interval solar tracking algorithm and the proposed algorithm were simulated for different number of mean daily re-orientations. The number of mean daily re-orientations was considered on a yearly basis. Figure 5 shows the increase in the received radiation in the developed open loop tracking device compared with a fixed system with latitude tilt. In Figure 5 the red line represents the gain of the fixed time interval algorithm over the fixed system. The green line represents the gain of the proposed algorithm over the fixed system.

As observed, for a mean number of daily reorientations greater than 5, there is less than 1.5% increase in the gain in relation to surfaces with latitude tilt and no significant difference between the two algorithms.

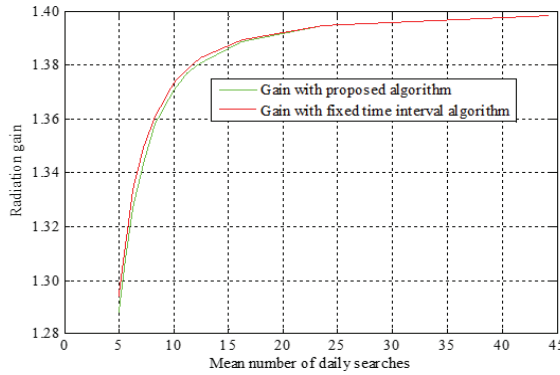


Figure 5. Radiation gain as a function of mean number of daily searches for the fixed time interval open loop algorithm and the proposed open loop algorithm over a fixed surface with latitude tilt.

For both algorithms the increase in the performance over the surface with latitude tilt was between 28 and almost 40% as the mean number of daily searches, N , varied from 5 to 44, which is in accordance with literature (Kelly & Gibson, 2009). It was observed that, when the number of mean daily searches was around 5, the fixed time interval algorithm performed better, but as the number of searches increased, the difference decreased, until, for N bigger than 23 the proposed algorithm started performing better. In that case, the differences between them were never bigger than 0.1%. Then, the reorientation criteria was fixed at $d \leq 22^\circ$ and the gain over the year was evaluated.

Figure 6 shows the variation of the incident radiation for the cases of fixed horizontal and surface with latitude tilt, just as for both tracking systems, for both equinoxes and solstices. Again, the difference between both algorithms was negligible.

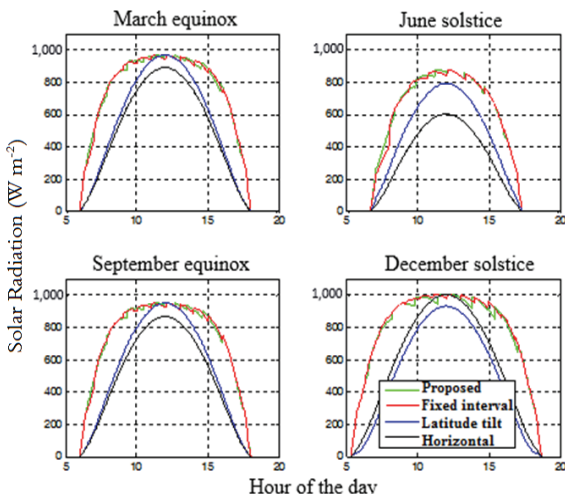


Figure 6. Radiation on solstices and equinoxes for horizontal, latitude tilted, fixed time interval open loop tracking and tracking with the proposed open loop algorithm for the city of Rio das Ostras, 22.49°S, Brazil.

Then, the yearly radiation gain was simulated for the locations described in the methodology and, once again, no significant difference was observed between the fixed time interval and the proposed open loop algorithms, as shown in Figure 7.

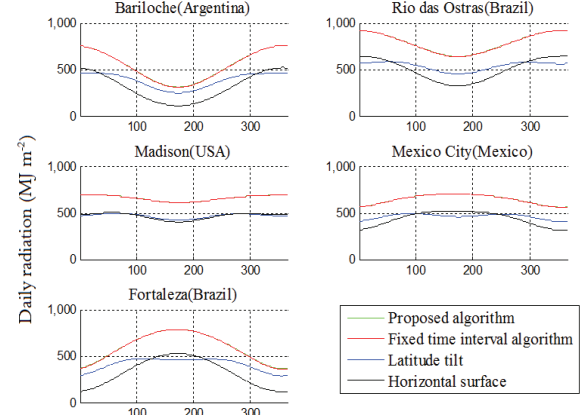


Figure 7. Radiation throughout the year for five different locations for horizontal surface, with latitude tilted surface, fixed time interval open loop tracking and tracking with the proposed open loop algorithm.

There was a small increase in the gain of the proposed algorithm, compared to the fixed time interval algorithm, as the location is farther away from the equator. The results are about 1.4 % higher for latitudes around 40° N or S.

A view of one of the constructed prototypes can be seen in Figure 8. It is able to move in slopes ranging between 0 and 90° degrees and up to 200° degrees in the azimuth.



Figure 8. Flat panel tracker prototype.

Power consumption occurs only during the movements of the prototypes and it does not consume energy while static. The tracker specifications are compiled in Table 4.

Table 4. Tracker prototype specifications.

Parameter	Value
Mean energy consumption	1 W h ⁻¹
Maximum angular speed	120° s ⁻¹
Maximum load	0.250 kg

Solar radiation measured between August/28/2013 and January/06/2014 can be seen in Figure 9 and 10. The data were measured every minute and their simple average was used to obtain the hourly radiation. Solar radiation variability caused by the presence of clouds can be observed in these figures.

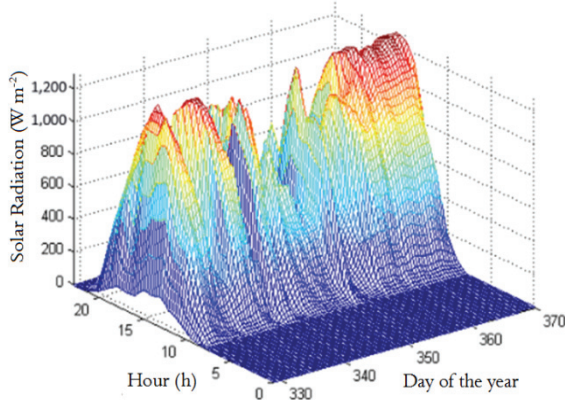


Figure 9. Incident solar radiation between Aug. /28/ 2013 and Nov. /25/ 2013 for the city of Rio das Ostras, Brazil, 22.49° S.

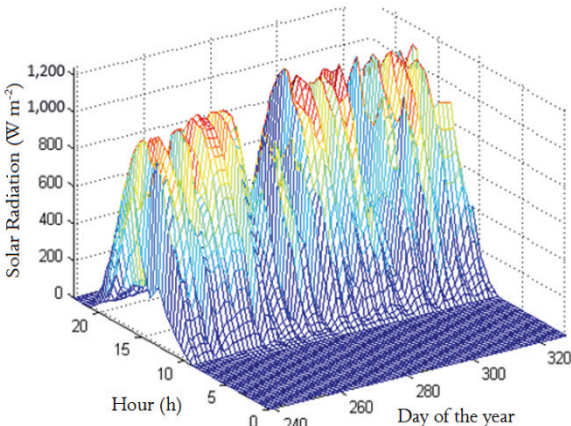


Figure 10. Incident solar radiation between Nov. /26/ 2013 and Jan. /06/ 2014 for the city of Rio das Ostras, Brazil, 22.49° S.

The experiments occurred on selected days under different sky conditions. The selected days and their sky conditions are shown in Table 5 and the generators output power for these days are shown in Figure 11.

By integrating the generated power throughout the measurement period and dividing it by the respective time interval, it was possible to compare

the average gains of the different systems. An average gain of 28.5% was obtained by the open loop system in relation to a fixed system with latitude tilt, while 33.0% was achieved by the closed loop system in relation to the fixed system.

Table 5. Experimentation day and cloudiness condition (National Institute of Meteorology [INMET], 2014).

Selected day	Condition
September/14/2013	Clear sky
November/30/2013	Clear sky
December/10/2013	Few clouds
December/26/13	Few clouds
August/29/2013	Mostly cloudy
September/18/2013	Mostly cloudy
October/28/2013	Mostly cloudy
September/01/2013	Considerable cloudiness
September/10/2013	Considerable cloudiness
September/23/2013	Considerable cloudiness
September/05/2013	Cloudy
October/30/2013	Cloudy
November/07/2013	Cloudy

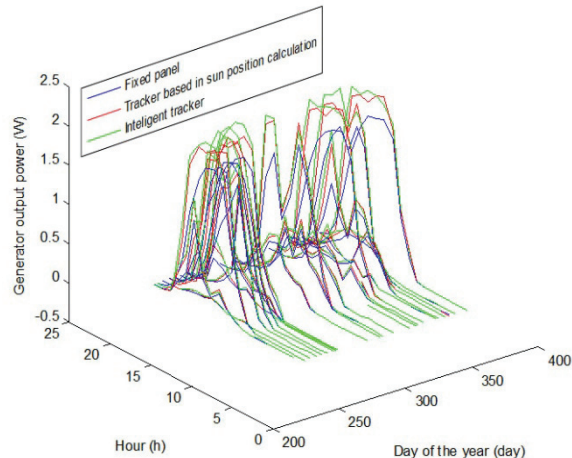


Figure 11. Generator output power on the selected days.

Conclusion

The proposed open loop solar tracking algorithm was compared to a fixed time interval open loop algorithm through two sets of simulations. The simulations showed that both algorithms have about the same increase in the received radiation, with a difference between them under 1.5% for all cases. The performance of photovoltaic generation systems with open loop, closed loop, latitude tilt and horizontal fixed systems was measured for 25 selected days comprising different cloudiness conditions. In most cases, the closed loop tracker showed higher efficiency than the open loop tracking system, with an average gain of 33.0 % over the energy produced by a fixed latitude tilted surface, in comparison with 28.5 % for the open loop tracking system.

Acknowledgements

The authors are thankful to the Universidade Federal de Viçosa, Minas Gerais States, CAPES, FAPEMIG and CNPq for all financial, technical and scientific support provided to this work.

References

Campbell Scientific. (2013). *CMP3-L Specifications and Technical Data*. Retrieved from <https://www.campbellsci.com/cmp3-l-specifications>

Chin, C. S., Babu, A., & McBride, W. (2011). Design, modeling and testing of a standalone single axis active solar tracker using MATLAB/Simulink. *Renewable Energy*, 36(11), 3075-3090.

Duffie, J. A., & Beckman, W. A. (2006). *Solar engineering of thermal processes*. Hoboken, NJ: John Wiley and Sons.

Electrical Electronic Corp [TES]. (2013). *TES-1333/1333R Solar Power Meter*. Retrieved from <http://tes.com.tw/1333e.htm>

Electrical Energy Research Center [EERC]. (2000). *Solarimetric Atlas from Brazil: terrestrial database*. Rio de Janeiro, RJ: Eletrobras.

Gómez-Gil, F. J., Wang, X., & Barnett, A. (2012). Energy production of photovoltaic systems: Fixed, tracking, and concentrating. *Renewable and Sustainable Energy Review*, 16(1), 306-313.

Guo, Y., Cha, J., Liu, W., & Tian Y. (2010). A system modeling method for optimization of a single axis solar tracker. *IEEE: International Conference on Computer Application and System Modeling*, 11(1), 30-34.

Hession, P. J., & Bonwick, W. J. (1984). Experience with a sun-tracker system. *Solar Energy*, 32(1), 3-11.

Kelly, N. A., & Gibson, T. L. (2011). Increasing the solar photovoltaic energy capture on sunny and cloudy days. *Solar Energy*, 85(1), 111-125.

Kelly, N. A., & Gibson, T. L. (2009). Improved photovoltaic energy output for cloudy conditions with a solar tracking system, *Solar Energy*, 83(11), 2092-2102.

Lubitz, W. D. (2010). Effect of manual tilt adjustments on incident irradiance on fixed and tracking solar panels, *Applied Energy*, 88(5), 1710-1719.

Mousazadeh H., Alireza K., Arzhang J., Hossein M., Karen A., & Ahmad S. (2009). A review of principle and sun-tracking methods for maximizing solar systems output. *Renewable and Sustainable Energy Reviews*, 13(8), 1800-1818.

National Institute of Meteorology. (2014). *Conventional stations database*. Retrieved from <http://www.inmet.gov.br/portal/index.php?r=estacoes/estacoesConvencionais>

Prapas, D. E., Norton, B., & Proebert, S. D. (1986). Sensor system for aligning a single-axis tracker with direct solar insolation. *Applied Energy*, 25(1), 1-8.

Renewable Energy Policy Network for the 21st Century. (2016). *Renewables 2016 Global Status Report*. Paris, FR: REN21 Secretariat. Retrieved from <http://www.ren21.net/status-of-renewables/global-status-report/>

Wollmann, C. A., & Sartori, M. G. B. (2010). Variação mensal e sazonal da nebulosidade em Santa Maria, Rio Grande do Sul, no período de 1969 a 2005. *Revista Geografar*, 5(2), 32-42.

Yilmaz, S., Ozcalik, H.R., Dogmus, O., Dincer, F., Akgol, O., & Karaaslan, M. (2015). Design of two axes sun tracking controller with analytically solar radiation calculations. *Renewable and Sustainable Energy Reviews*, 43(C), 997-1005.

Zogbi R., & Laplaze, D. (1984). Technical note: design and construction of a sun tracker. *Solar Energy*, 33(1), 369-372.

Received on September 24, 2015.

Accepted on July 29, 2016.

License information: This is an open-access article distributed under the terms of the Creative Commons Attribution License, which permits unrestricted use, distribution, and reproduction in any medium, provided the original work is properly cited.